

## $D_s \rightarrow \eta(\prime)$ semi-leptonic decay form factors

---

**Sara Collins, Issaku Kanamori\* and Johannes Najjar**

*Institut für Theoretische Physik, Universität Regensburg, 93040 Regensburg, GERMANY*

*E-mail:* sara.collins@physik.uni-regensburg.de,

issaku.kanamori@physik.uni-regensburg.de,

johannes.najjar@physik.uni-regensburg.de

We report on our on-going study of the  $D_s$  to  $\eta(\prime)$  semi-leptonic decay form factors with  $n_f = 2+1$  configurations. We include disconnected fermion loop diagrams, which give large contributions to the  $D_s$  to  $\eta'$  form factor.

*31st International Symposium on Lattice Field Theory LATTICE 2013*

*July 29 August 3, 2013*

*Mainz, Germany*

---

\*Speaker.

## 1. Introduction

The semi-leptonic decay  $D_s \rightarrow l\bar{\nu}_l\eta^{(\prime)}$  carries information about  $\eta$ - $\eta'$  mixing so that the investigation of this mode helps to understand the mixing angle and also possible gluonic contributions [1]. For decays involving  $\eta'$ , the chiral anomaly should play some role and it is an interesting playground for obtaining a deeper understanding of the quantum field theory. There are no published results on the form factors from the lattice, while predictions from light cone QCD sum rule [2, 3] are available.

The relevant matrix element for these decay modes is

$$\langle \eta^{(\prime)}(k) | V^\mu(q^2) | D_s(p) \rangle = f_+(q^2) \left[ (p+k)^\mu - \frac{M_{D_s}^2 - M_{\eta^{(\prime)}}^2}{q^2} q^\mu \right] + f_0(q^2) \frac{M_{D_s}^2 - M_{\eta^{(\prime)}}^2}{q^2} q^\mu, \quad (1.1)$$

where  $V^\mu$  is a vector current and  $M_{D_s}$  and  $M_{\eta^{(\prime)}}$  are the masses of the  $D_s$  and  $\eta^{(\prime)}$ , respectively. This matrix element is characterized by two form factors,  $f_0(q^2)$  and  $f_+(q^2)$ . So far, we have focused on the scalar form factor  $f_0(q^2)$ , which we can also obtain from a scalar current  $S = \bar{s}c$ ,

$$f_0(q^2) = \frac{m_c - m_s}{M_{D_s}^2 - M_{\eta^{(\prime)}}^2} \langle \eta^{(\prime)} | S | D_s \rangle. \quad (1.2)$$

We use this relation because the combination  $(m_c - m_s)S$  (and therefore  $f_0(q^2)$ ) does not receive renormalization due to the partially conserved vector current [4].

The three point function needed to compute the form factor contains fermion disconnected loops, shown pictorially here:

$$\langle \eta^{(\prime)}(\vec{k}) | S(\vec{q}) | D_s(\vec{p}) \rangle = \text{Diagram 1} - \sum_{l=u,d,s} \left( \text{Diagram 2} + \text{Diagram 3} \right). \quad (1.3)$$

The disconnected loops should be summed over three light flavors which enhances the magnitude roughly by a factor of three. These loops contain the contributions from the chiral anomaly to the  $\eta'$ -meson. For these reasons, the disconnected loops may contribute significantly. As already reported in [5, 6], the calculation is feasible and the contributions are indeed significant.

We use QCDSF  $n_f = 2 + 1$  configurations [7, 8]. The actions are the tree level Symanzik improved action for the gluon and the non-perturbative stout link improved clover action for the quarks. We use the same action for the valance charm quark with the mass tuned to give the physical mass of the  $1S$  spin averaged charmonium state. The  $u$ -,  $d$ - and  $s$ - quark masses are tuned so that their average  $\frac{1}{3}(m_u + m_d + m_s)$  is fixed and that  $2M_K^2 + M_\pi^2$  coincides with the physical values. At the SU(3) flavor symmetric point we have  $m_{u,d} = m_s$ , and in taking the chiral limit we reduce  $m_{u,d}$  and increase  $m_s$  with their average fixed. Due to this strategy of choosing quark masses, it is natural to treat  $\eta$  and  $\eta'$  using the SU(3) flavor octet-singlet basis. The lattice size we have used so far is  $24^3 \times 48$  and the lattice spacing is  $a \simeq 0.08$  fm. We used 939 configurations at the SU(3) flavor symmetric point ( $M_\pi \simeq 450$  MeV) and 239 configurations with lighter  $u/d$  quarks ( $M_\pi \simeq 348$  MeV).

The most computationally expensive quantity to calculate is the fermion one point loop,

$$\mathcal{C}_{1\text{pt}}^f(t, \vec{k}) = \sum_{\vec{x}} \exp(i\vec{k} \cdot \vec{x}) \text{tr} \left[ \sum_{\vec{x}', \vec{x}''} \gamma_5 \phi(\vec{x}, \vec{x}'') M_f^{-1}(t, \vec{x}''; t, \vec{x}') \phi(\vec{x}', \vec{x}) \right] = \text{Diagram 4}, \quad (1.4)$$

where  $M_f$  is the Dirac operator for flavor  $f$  and  $\phi(\vec{x}, \vec{x}')$  is a smearing function. We combined the stochastic estimation with low mode averaging (with 24 or 40 eigen modes), hopping parameter acceleration, spin and time dilution (non-zero stochastic noise on every 4 time slices), and the truncated solver method [9].

The low eigenmodes of the light and strange quarks calculated for  $\mathcal{C}_{1\text{pt}}^f$  were also used for the low mode averaging of the connected two point functions, and for a similar trick for the disconnected three point functions. We used the stochastic method to obtain the connected three point function, which has an advantage over the other methods since it enables us to access many momentum combinations at a relatively lower cost [10].

## 2. Extracting $\eta$ and $\eta'$ states

To calculate the matrix element (1.3), we first need to build the interpolating operators for the  $D_s$  and the  $\eta^{(\prime)}$  meson. The operator for the  $D_s$  is easy to obtain but ones for  $\eta^{(\prime)}$  are non-trivial due to the mixing. We start with SU(3) octet-singlet basis,  $\eta_8 = \frac{1}{\sqrt{6}}(u\bar{u} + d\bar{d} - 2s\bar{s})$  and  $\eta_1 = \frac{1}{\sqrt{3}}(u\bar{u} + d\bar{d} + s\bar{s})$ . We can build the following  $2 \times 2$  two-point correlation function by using smeared interpolating operators  $\mathcal{O}_8$  for the octet and  $\mathcal{O}_1$  for the singlet:

$$C_2(t; \vec{k}) = \begin{pmatrix} \langle \mathcal{O}_8(t; \vec{k}) \mathcal{O}_8^\dagger(0) \rangle & \langle \mathcal{O}_8(t; \vec{k}) \mathcal{O}_1^\dagger(0) \rangle \\ \langle \mathcal{O}_1(t; \vec{k}) \mathcal{O}_8^\dagger(0) \rangle & \langle \mathcal{O}_1(t; \vec{k}) \mathcal{O}_1^\dagger(0) \rangle \end{pmatrix}. \quad (2.1)$$

Here,  $t$  is the sink-source time separation and the operators at the sink are projected on to momentum  $\vec{k}$ . Each element of eq. (2.1) contains both connected and disconnected fermion loop contributions. We made use of the translational invariance in the time direction to calculate the disconnected two point function.

The diagonalized two point functions give the  $\eta$  and  $\eta'$  two point functions. The eigenvectors, which can be parameterized by one mixing angle  $\theta$ , give interpolating operators for  $\eta$  and  $\eta'$ :

$$\mathcal{O}_\eta = \cos \theta \mathcal{O}_8 - \sin \theta \mathcal{O}_1, \quad \mathcal{O}_{\eta'} = \sin \theta \mathcal{O}_8 + \cos \theta \mathcal{O}_1. \quad (2.2)$$

The mixing angle above corresponds to a mixing between the interpolating operators and is not the mixing of the physical observable. In the SU(3) flavor symmetric case, there is no mixing so the  $\eta'$  is purely  $\eta_1$  and the  $\eta$  is purely  $\eta_8$ . The effective masses after applying an improvement described below are plotted in Fig. 1.

We can improve the measurement of the mass using a relation for the finite volume effects. For simplicity, let us consider the SU(3) flavor symmetric case, in which the  $\eta'$  is purely  $\eta_1$ . It is well-known that the mass of  $\eta'$  is sensitive to the fluctuation of the topological charge. In the extreme case at fixed topology, the correlation function for the topological charge density  $\rho(x)$  tends to a constant for large separation [11]

$$\langle \rho(x) \rho(0) \rangle_Q \xrightarrow{|x| \rightarrow \infty} -\frac{1}{V_4} \left( \frac{Q^2}{V_4} - \chi_t \right) + \dots, \quad (2.3)$$

where  $\chi_t$  is the topological susceptibility and the expectation value is taken in a sector of topological charge fixed to  $Q$ . This correlation function is essentially the  $\eta'$  two point function. The above

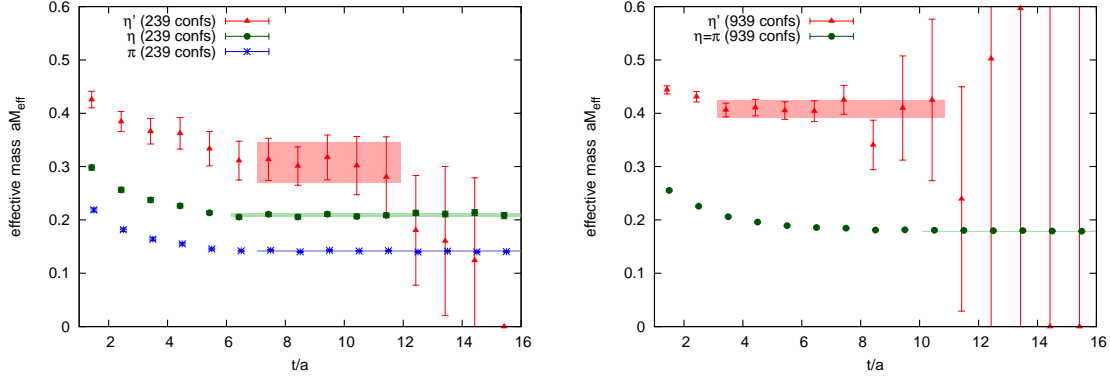


**Figure 1:** Effective mass plot of  $\eta'$  and  $\eta$ . For comparison, the effective mass of the  $\pi$  is also plotted. Left panel:  $M_\pi = 348 \text{ MeV}$  case. Right panel:  $M_\pi = 450 \text{ MeV}$  case (SU(3) flavor symmetric), where  $\pi = \eta = \eta_8$  and  $\eta' = \eta_1$ . Fits were obtained without using the dispersion relation.

expression assumes that the full  $Q$  fluctuation is Gaussian and that the higher terms in  $1/V_4$ , the inverse four-volume, are negligible.

Eq. (2.3) implies that for finite statistics, where the  $Q$ -distribution deviates from the true distribution due to the statistical fluctuations, one may observe the remnant of the constant part in the  $\eta'$  two-point function for  $\vec{k} = \vec{0}$ . This is indeed the case for the SU(3) symmetric point. We could simply remove the constant part by fitting. We used, however, an improved observable as follows. Noting that the topological charge can also be obtained from the pseudo-scalar density, we can relate it to a disconnected fermion loop of flavor  $l$  ( $= u = d = s$ ),  $\mathcal{C}_{1\text{pt}}^l$ :

$$Q = \frac{1}{\alpha} \sum_x \mathcal{C}_{1\text{pt}}^l(x) = \frac{1}{\alpha} \sum_t \mathcal{C}_{1\text{pt}}^l(t, \vec{k} = \vec{0}) = \frac{1}{\alpha} \sum_x \text{Tr} \left[ \gamma_5 \text{loop}^l \right] \equiv \frac{1}{\alpha} Q_l, \quad (2.4)$$

where  $\alpha$  depends on the quark mass  $m_l$  and the renormalization. We used eq. (2.3) and (2.4) to reduce a  $Q$ -dependent fluctuation in the two point function:

$$\left\langle \mathcal{O}_1(t; \vec{k} = \vec{0}) \mathcal{O}_1^\dagger(0) - \frac{3}{TV_4} Q_l^2 \right\rangle \xrightarrow{t \rightarrow \infty} \frac{|Z_{\eta_1}|^2}{2M_{\eta_1}} \exp(-M_{\eta_1} t) + \alpha^2 \frac{3\chi_t}{TV_4} + \dots, \quad (2.5)$$

where  $T$  is the lattice size in the time direction and  $Z_{\eta_1} = \langle \eta_1 | \mathcal{O}_{\eta_1} | 0 \rangle$ . Fitting the above with a functional form of  $A \exp(-M_{\eta_1} t) + B$ , gives a better estimation of  $M_{\eta_1}$ . This method applies only in the  $\vec{k} = \vec{0}$  case, since the Fourier transformation of the r.h.s in eq. (2.3) vanishes for  $\vec{k} \neq \vec{0}$ . The effective mass with and without the improvement are plotted in Fig. 2.

Finally we combined the non-zero momentum data and the dispersion relation. In Fig. 3, we plot the energy at momentum  $\vec{k}$  and the fitted dispersion relation. Even after the improvement described here, the  $\vec{k} = \vec{0}$  data has a larger error than some of the  $\vec{k} \neq \vec{0}$  data. We applied a similar improvement to the  $m_l \neq m_s$  case. For this ensemble, we did not observe a significant constant term in the two point function before the improvement, however, subtracting the corresponding of the  $Q_l^2$  term in eq. (2.5) significantly reduced the statistical fluctuations.

### 3. Results

Having obtained the interpolating operators (2.2), we can construct the three point function

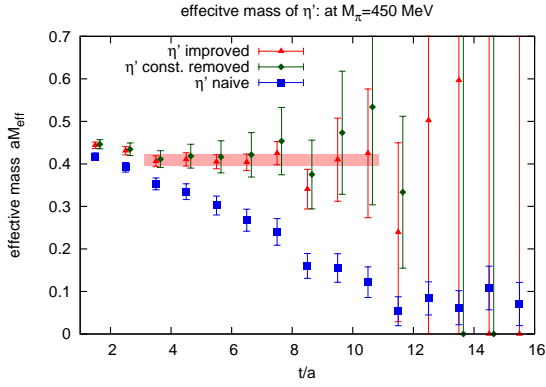


**Figure 2:** Effective mass of the  $\eta'$  at SU(3) symmetric point. The naive plot (blue square) is affected by the remnant constant, while the improved one (red triangle) shows a clear plateau. The plot with the remnant constant removed but without using eq. (2.5)(green diamond) has a larger error.

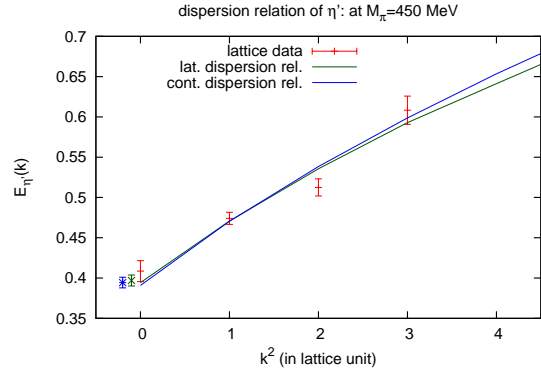


**Figure 3:** Spectrum and fitted dispersion relation of  $\eta'$ . Both lattice and continuum relations give the same result within the error. To improve visibility, the resulting masses from the dispersion relation are slightly shifted to the left.

needed for the form factor:

$$\begin{aligned}
 C_{3\text{pt}}(t, \vec{p}, \vec{q}, \vec{k}) &= \langle 0 | \mathcal{O}_{\eta^{(\prime)}}(\vec{k}, t_{\text{sep}}) S(\vec{q}, t) \mathcal{O}_{D_s}^\dagger(\vec{p}, 0) | 0 \rangle \\
 &= \frac{Z_{\eta^{(\prime)}}}{2E_{\eta^{(\prime)}}} \frac{Z_{D_s}}{2E_{D_s}} \exp[-E_{D_s}t - E_{\eta^{(\prime)}}(t_{\text{sep}} - t)] \times \left[ \langle \eta^{(\prime)}(\vec{k}) | S(\vec{q}) | D_s(\vec{p}) \rangle + \dots \right], \quad (3.1)
 \end{aligned}$$

where  $t_{\text{sep}}$  is the sink-source separation. By fitting the two point function

$$C_{2\text{pt}}^{D_s}(t, \vec{p}) = \frac{|Z_{D_s}|^2}{2E_{D_s}} \exp[-E_{D_s}t] + \dots \quad (3.2)$$

for the  $D_s$  and similar ones for the  $\eta$  and the  $\eta'$ , we obtained  $Z_{D_s}$  and  $E_{D_s}$  etc, which allowed us to extract the matrix element  $\langle \eta^{(\prime)}(\vec{k}) | S(\vec{q}) | D_s(\vec{p}) \rangle$  from eq. (3.1). Thus, using eq. (1.2) we computed the scalar form factor  $f_0(q^2)$  from the matrix elements. As we will discuss below, we removed excited contributions and obtained the matrix elements between the ground states. The preliminary results are plotted in Fig. 4, where the errors were obtained from a jackknife analysis. We fit the results with one pole functions,  $f_0(q^2) = f_0(0)/(1 - bq^2)$ . The preliminary values at zero momentum transfer are  $f_0^{D_s \rightarrow \eta}(0) = 0.52(2)$  and  $f_0^{D_s \rightarrow \eta'}(0) = 0.42(4)$  for the SU(3) symmetric case,  $f_0^{D_s \rightarrow \eta}(0) = 0.59(5)$  and  $f_0^{D_s \rightarrow \eta'}(0) = 0.41(5)$  for the  $M_\pi = 348 \text{ MeV}$  case.

To extract the matrix element between the ground state of  $D_s$  and  $\eta^{(\prime)}$ , it is important to remove the excited contributions. We tuned the smearing to suppress the excited contributions, however, some residual pollution of the three point function remains. If we could take  $t_{\text{sep}}$  and  $t$  large enough, the residual pollution would be negligible. We cannot use such large  $t_{\text{sep}}$  and  $t$  since the statistical errors become unreasonably large. After removing the leading exponential factors by taking a ratio,

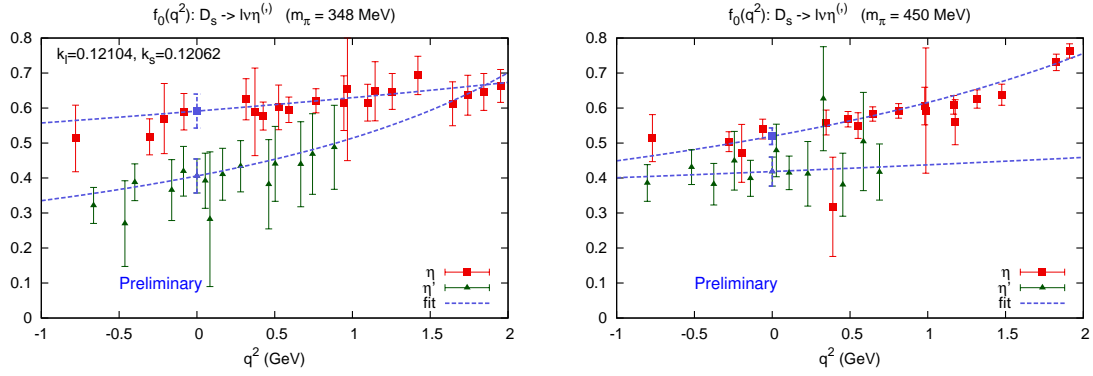


**Figure 4:** Preliminary results for the scalar form factor  $f_0(q^2)$ , at the  $M_\pi = 348$  MeV point (left panel) and the SU(3) flavor symmetric point (right panel).

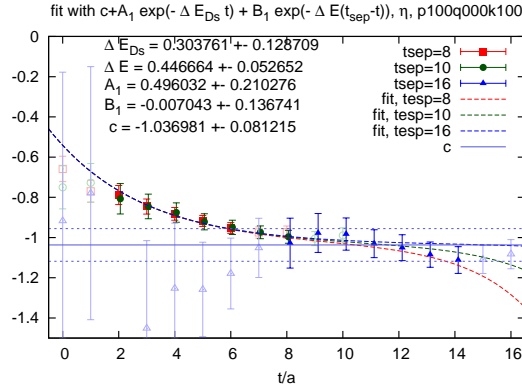


**Figure 5:** Fit of  $R(t)$  with excited contributions from  $D_s$  and  $\eta$ , from the  $M_\pi = 348$  MeV ensemble.  $D_s(\vec{p} = (1, 0, 0))$  is located at  $t/a = 0$  and  $\eta(\vec{k} = (1.0, 0))$  is at  $t/a = 8, 10$  and  $16$ . The data points with open symbols were not used in the fitting.

we have

$$\begin{aligned}
 R(t) &\equiv \frac{C_{3\text{pt}}(t, \vec{p}, \vec{q}, \vec{k})}{\frac{Z_{\eta^{(\prime)}}}{2E_{\eta^{(\prime)}}} \frac{Z_{D_s}}{2E_{D_s}} \exp(-E_{D_s}t - E_{\eta^{(\prime)}}(t_{\text{sep}} - t))} \\
 &= \langle \eta^{(\prime)}(\vec{k}) | S(\vec{q}) | D_s(\vec{p}) \rangle + A_1 \exp(-\Delta E_{D_s}t) + B_1 \exp(-\Delta E_{\eta^{(\prime)}}(t_{\text{sep}} - t)) + \dots, \quad (3.3)
 \end{aligned}$$

where  $\Delta E_{D_s}$  and  $\Delta E_{\eta^{(\prime)}}$  are the energy gaps to the first excited state. We simultaneously fit the ratio (3.3) with three different  $t_{\text{sep}}/a = (8, 10, 16)$  (for  $\eta$  in the SU(3) symmetric point, we also used  $t_{\text{sep}}/a = 24$ ) by three terms in the r.h.s., using the energy gaps obtained from the two point functions. If the two point function did not allow us to extract  $\Delta E_{\eta^{(\prime)}}$ , we used the first two terms, only, in eq. (3.3). A typical example of the fitting is shown in Fig.5. The plot shows that the ratio is described well by our fit ansatz.

#### 4. Conclusions

The lattice calculation of semi-leptonic decay form factors for  $D_s \rightarrow l \bar{\nu} \eta$  and  $D_s \rightarrow l \bar{\nu} \eta'$  are

feasible, including the disconnected fermion loop contributions. This is the first lattice result for these form factors and we can obtain the scalar form factor  $f_0(q^2)$  at  $q^2 = 0$  with 10–15% statistical error at  $M_\pi \simeq 450$  and 348 MeV.

We are planning to calculate the other form factor  $f_+(q^2)$ , which requires a renormalization factor. Other targets are the form factors corresponding to the decay into  $\phi$ , for which a rigorous treatment requires disconnected fermion contributions. The mixing of  $\eta$  and  $\eta'$ , and its quark mass dependence are also interesting.

### Acknowledgements

This work was supported by the DFG (SFB/TRR 55) and the EU (ITN STRONGnet). We used a modified version of the CHROMA software suite [12]. We used time granted by PRACE at Fermi in CINECA, as well as the Athene HPC cluster and iDataCool at the University of Regensburg. We thank G. S. Bali, S. Dürr, B. Gläbtle, E. Gregory, C. McNeile, P. Pérez-Rubio and A. Schäfer for discussions.

### References

- [1] C. Di Donato, G. Ricciardi and I. Bigi,  $\eta - \eta'$  Mixing - From electromagnetic transitions to weak decays of charm and beauty hadrons, Phys. Rev. D **85** (2012) 013016 [arXiv:1105.3557 [hep-ph]].
- [2] K. Azizi, R. Khosravi and F. Falahati, Exclusive  $D_s \rightarrow (\eta, \eta')lv$  decays in light cone QCD, J. Phys. G **38** (2011) 095001 [arXiv:1011.6046 [hep-ph]].
- [3] N. Offen, F. A. Porkert and A. Schaefer, Light-Cone Sum Rules for the  $D_{(s)} \rightarrow \eta^{(\prime)}lv_l$  Form Factor, Phys. Rev. D **88** (2013) 034023 [arXiv:1307.2797 [hep-ph]].
- [4] H. Na, C. T. H. Davies, E. Follana, G. P. Lepage and J. Shigemitsu, The  $D \rightarrow K, lv$  Semileptonic Decay Scalar Form Factor and  $|V_{cs}|$  from Lattice QCD, Phys. Rev. D **82** (2010) 114506 [arXiv:1008.4562 [hep-lat]].
- [5] G. S. Bali *et al.* [QCDSF Collaboration], Disconnected contributions to  $D$ -meson semi-leptonic decay form factors, PoS LATTICE **2011** (2011) 283 [arXiv:1111.4053 [hep-lat]].
- [6] I. Kanamori, Lattice calculations of  $D_s$  to  $\eta$  and  $\eta'$  decay form factors, PoS ConfinementX (2012) 143 [arXiv:1302.6087 [hep-lat]].
- [7] W. Bietenholz *et al.* [QCDSF collaboration], Tuning the strange quark mass in lattice simulations, Phys. Lett. B **690** (2010) 436 [arXiv:1003.1114 [hep-lat]].
- [8] W. Bietenholz *et al.* [QCDSF collaboration], “Flavour blindness and patterns of flavour symmetry breaking in lattice simulations of up, down and strange quarks,” Phys. Rev. D **84** (2011) 054509 [arXiv:1102.5300 [hep-lat]].
- [9] G. S. Bali, S. Collins and A. Schäfer, Effective noise reduction techniques for disconnected loops in Lattice QCD, Comput. Phys. Commun. **181** (2010) 1570 [arXiv:0910.3970 [hep-lat]].
- [10] R. Evans, G. Bali and S. Collins, Improved Semileptonic Form Factor Calculations in Lattice QCD, Phys. Rev. D **82** (2010) 094501 [arXiv:1008.3293 [hep-lat]].
- [11] S. Aoki, H. Fukaya, S. Hashimoto and T. Onogi, Finite volume QCD at fixed topological charge, Phys. Rev. D **76** (2007) 054508 [arXiv:0707.0396 [hep-lat]].
- [12] R. G. Edwards and B. Joó [SciDAC and LHPC and UKQCD Collaborations], The Chroma software system for lattice QCD, Nucl. Phys. Proc. Suppl. **140** (2005) 832 [hep-lat/0409003].